



## Advanced conjugate gradient technique for image restoration

Basim Abbas Hassan<sup>1,\*</sup>, Saif A. Hussein<sup>2</sup>, and Ayad Abdulaziz Mahmood<sup>3</sup>

<sup>1</sup>Department of Mathematic, College of Computers Sciences and Mathematics, University of Mosul, Iraq.

<sup>2</sup>Salladdin in Education Directorate, Tikrit, Iraq.

<sup>3</sup>Department of Statistics and Information Techniques Technical, College of Management, Northern Technical University, Mosul.

### Abstract

In this study, a novel conjugate coefficient that is especially intended to address picture restoration issues is presented within the context of the conjugate gradient approach. Stability and dependability are ensured throughout the iterative process by the suggested method, which not only ensures global convergence but also upholds the crucial descent feature. The results of extensive numerical studies show that the new method regularly performs better than conventional tactics. Significant gains in computing efficiency and restoration accuracy are particularly evident when compared to the traditional Fletcher-Reeves (FR) conjugate gradient approach. With better performance in iteration reduction, function evaluations, and feature retention, our results show that the improved conjugate gradient approach is a reliable and efficient tool for high-quality picture reconstruction.

**Keywords.** Advanced conjugate gradient formula, Convergence analysis, Impulse noise removal in images.

**2010 Mathematics Subject Classification.** 90C30, 49M37, 68U10.

### 1. INTRODUCTION

Since nonlinear optimization problems, which are sometimes of considerable size, arise from many real-world applications, first-order techniques are particularly suitable. Gradient-based techniques have proven to be particularly effective in this class for solving complex image processing problems, whether they are unrestricted or have limits [9, 10].

Let  $x$  be the original image of  $M \times N$  pixels, with  $A = \{1, 2, 3, \dots, M\} \times \{1, 2, 3, \dots, N\}$  as the index set. The damaged image with salt-and-pepper impulse noise is represented by  $y$ , whereas the image recovered with the median filter is shown by  $\tilde{y}$ . The restoration method's objective is to alter each pixel  $x_{i,\check{j}}$ , where  $\tilde{y}_{i,\check{j}}$  is the pixel that the filtering procedure was able to restore. By considering the neighbourhood  $V_{i,\check{j}}$  of  $x_{i,\check{j}}$ , the median filter suppresses the impulsive noise represented by the extreme values  $s_{max}$  and  $s_{min}$ , which establish the dynamic range of the original image [3]. The noisy pixel index set is defined as  $N = \left\{ (i, \check{j}) \in A / \tilde{y}_{i,\check{j}} \neq y_{i,\check{j}}, y_{i,\check{j}} = s_{max} \text{ or } s_{min} \right\}$  and its corresponding  $N^c = \left\{ (i, \check{j}) \in A / (i, \check{j}) \notin N \right\}$ . Therefore, the median filtering procedure is used in the first stage to identify noisy pixels. A noisy pixel is represented as  $x_{i,\check{j}}$  for every  $(i, \check{j}) \in N$ , where  $c = |N|$  is the total number of noisy pixels and  $u = \left[ u_{i,\check{j}} \right]_{(i,\check{j}) \in N} \in R^c$  is the equivalent vector.  $S_{i,\check{j}}^1 = 2 \sum_{(m,n) \in V_{i,\check{j}} \cap N^c} \phi_\omega(u_{i,\check{j}} - y_{m,n})$ ,  $S_{i,\check{j}}^2 = \sum_{(m,n) \in V_{i,\check{j}} \cap N} \phi_\omega(u_{i,\check{j}} - y_{m,n})$  is defined by the edge-preserving function  $\phi_\omega$ . The second stage is to solve an unconstrained optimisation problem for impulse noise reduction, in accordance with [26]

$$\text{Min} f_\omega(u) = \sum_{(i,\check{j}) \in N} \left[ \left| u_{i,\check{j}} - y_{i,\check{j}} \right| + \frac{\gamma}{2} \left( 2S_{i,\check{j}}^1 + S_{i,\check{j}}^2 \right) \right]. \quad (1.1)$$

Received: 28 November 2025; Accepted: 26 February 2026.

\* Corresponding author. Email: basimah@uomosul.edu.iq.

where  $\gamma > 0$  is the regularisation parameter governing the level of smoothing. Smoothness is promoted and edge preservation is guaranteed via the edge-preserving function  $\phi_\omega = \sqrt{u + \omega^2}$ , where  $\omega > 0$ .

The inclusion of the word  $|u_{i,\check{y}} - y_{i,\check{y}}|$  in Equation (1.1) has been demonstrated in earlier research [8, 14] to make the identification of noisy pixels easier. But in the process of restoring faulty pixels, this term may also add a slight bias. We initially identify the collection of noisy pixels in the first phase of our method. This phrase is therefore no longer needed in the next repair step. In order to concentrate just on the functional, which may be written as follows, we suggest eliminating it from Equation (1.1).

$$f_\alpha(u) = \sum_{(i,\check{y}) \in \Omega} \left[ (2 \times S_{i,\check{y}}^1 + S_{i,\check{y}}^2) \right]. \quad (1.2)$$

The efficiency of conjugate gradient (CG) methods, which are generally considered as potent iterative optimization approaches, is very advantageous for the task of impulsive noise elimination, [27]. Finding  $u^*$  that minimizes a smooth function is the goal:

$$f(u^*) = \min_{x \in R^N} f(u)f(u^*). \quad (1.3)$$

See, [15]. The typical iterative technique is used by the majority of conjugate gradient algorithms:

$$u_{\kappa+1} = u_\kappa + \alpha_\kappa d_\kappa u_{\kappa+1}, \quad (1.4)$$

where  $\alpha_\kappa$  denotes the step size. One common choice for  $\alpha_\kappa$ , as described in [24], is:

$$\alpha_\kappa = -\frac{g_\kappa^T d_\kappa}{d_\kappa^T Q d_\kappa} \alpha_\kappa. \quad (1.5)$$

In reality, a line search technique like the Wolfe criteria [13] is frequently used to find the step length  $\alpha_\kappa$ :

$$f(u_\kappa + \alpha_\kappa d_\kappa) \leq f(u_\kappa) + \delta \alpha_\kappa g_\kappa^T d_\kappa, \quad (1.6)$$

$$d_\kappa^T (u_\kappa + \alpha_\kappa d_\kappa) \geq \sigma d_\kappa^T g_\kappa, \quad (1.7)$$

where  $0 < \delta < \sigma < 1$ , see [4]. There has been a lot of interest in the convergence characteristics and usefulness of CG methods; more details are given in [17].

The search direction is modified in the following manner during the iteration process:

$$d_{\kappa+1} = -g_{\kappa+1} + \beta_\kappa d_\kappa, \quad (1.8)$$

where  $\beta_\kappa$  is a scalar parameter. Different numerical behaviors result from different  $\beta_\kappa$  selections. For instance, [6] provides the classical Fletcher–Reeves (FR) parameter:

$$\beta_\kappa^{FR} = \frac{\|g_{\kappa+1}\|^2}{\|g_\kappa\|^2}. \quad (1.9)$$

However, the FR approach may show sluggish convergence if the search direction is poorly chosen or the step size is too tiny. Because of these drawbacks, the FR method frequently exhibits subpar performance in numerical studies.

Several studies have examined the convergence properties of conjugate gradient (CG) algorithms [17, 23]. The pioneer in this subject, Zoutendijk [28], shown that using an accurate line search facilitates global convergence of the Fletcher–Reeves (FR) technique. Building on this basis, several more conjugate gradient parameter formulae have been created that provide better numerical performance together with assurances of global convergence. According to recent research on nonlinear conjugate gradient techniques, such as that conducted by Basim [17] and Hideaki and Yasushi [23], the following definitions of parameters are frequently used:

$$\beta_\kappa^{HY} = \frac{\|g_{\kappa+1}\|^2}{2/\alpha_\kappa(f_\kappa - f_{\kappa+1})}, \beta_\kappa^B = \frac{\|g_{\kappa+1}\|^2}{(f_\kappa - f_{\kappa+1})/\alpha_\kappa - g_\kappa^T d_\kappa/2}. \quad (1.10)$$

The class of conjugate gradient algorithms under consideration here, as documented in [7], effectively meets all the favourable characteristics and benefits anticipated from such iterative optimisation techniques while maintaining a high level of computing efficiency. The use of a quadratic model improves their performance even further by enabling



these techniques to take advantage of the underlying optimisation problem's structure. Particularly for unconstrained optimisation problems where numerical stability and quick convergence are crucial, our modelling method not only optimises the advantages of conventional conjugate gradient approaches but also greatly enhances their performance.

To improve performance for different problem contexts, several variants of the conjugate gradient technique have been developed, either by carefully adjusting the fundamental parameters or by expanding upon them. We have created a novel conjugate parameter in this study to help determine the direction of the search. This new parameter, which utilises the quadratic model, provides precise control over the search trajectory, ensuring both proper directionality and better convergence functionality. The approach is particularly suitable for complex unconstrained optimisation applications such as large-scale image restoration since it effectively balances robustness with computational economy.

## 2. CONJUGATING A NEW FORMULA

The objective function's Taylor series expansion yields the new conjugate gradient formula:

$$f(x) = f(x_{\kappa+1}) - g_{\kappa+1}^T s_{\kappa} + \frac{1}{2} s_{\kappa}^T Q(u_{\kappa+1}) s_{\kappa}, \quad (2.1)$$

where  $Q$  denotes the Hessian matrix. At iteration  $k + 1$ , the gradient may be written as follows:

$$g_{\kappa+1} = g_{\kappa} + Q(u_{\kappa+1}) s_{\kappa}. \quad (2.2)$$

We derive the relationship from these expressions:

$$s_{\kappa}^T Q(u_{\kappa}) s_{\kappa} = 1/2 y_{\kappa}^T s_{\kappa} + (f_{\kappa+1} - f_{\kappa}) - g_{\kappa}^T s_{\kappa}. \quad (2.3)$$

This makes the calculation possible:

$$d_{\kappa}^T Q(u_{\kappa}) s_{\kappa} = \alpha_{\kappa} (g_{\kappa}^T d_{\kappa})^2 / (1/2 y_{\kappa}^T s_{\kappa} + (f_{\kappa+1} - f_{\kappa}) - g_{\kappa}^T s_{\kappa}). \quad (2.4)$$

In order to enforce the conjugacy condition  $d_{\kappa+1}^T y_{\kappa} = 0$  for the modified search direction  $d_{\kappa+1}$ , the new conjugate parameter is defined as follows.

$$\beta_{\kappa} = \frac{g_{\kappa+1}^T Q s_{\kappa}}{d_{\kappa}^T Q s_{\kappa}}. \quad (2.5)$$

The result of replacing the prior relation is:

$$\beta_{\kappa} = \frac{g_{\kappa+1}^T y_{\kappa}}{\alpha_{\kappa} (g_{\kappa}^T d_{\kappa})^2 / (1/2 y_{\kappa}^T s_{\kappa} + (f_{\kappa+1} - f_{\kappa}) - g_{\kappa}^T s_{\kappa})}. \quad (2.6)$$

Applying exact line search in the above equation simplifies the expression to:

$$\beta_{\kappa} = \frac{\|g_{\kappa+1}\|^2}{\alpha_{\kappa} (g_{\kappa}^T d_{\kappa})^2 / (1/2 y_{\kappa}^T s_{\kappa} + (f_{\kappa+1} - f_{\kappa}) - g_{\kappa}^T s_{\kappa})}. \quad (2.7)$$

This serves as the foundation for our suggested approach, the BBJ algorithm. The algorithm works like this:

---

### Algorithm 1 Algorithm BBJ

---

- 1: **Initialization.** Given  $x_0 \in R^n$ , set  $k = 0$ ,  $d_0 = -g_0$ .
  - 2: **while true do**
  - 3:   **if**  $\|\nabla f(u_k)\| \leq \varepsilon$  **then**
  - 4:     **stop.**
  - 5:   **end if**
  - 6:   Apply steps (1.6) and (1.7) to calculate the step length  $\alpha_{\kappa}$ .
  - 7:   Compute  $\beta_{\kappa}$  using Equation (2.7).
  - 8:   update the search direction  $d_{\kappa+1} = -g_{\kappa+1} + \beta_{\kappa} d_{\kappa}$ .
  - 9:   Update  $x_{\kappa+1} = x_{\kappa} + \alpha_{\kappa} d_{\kappa}$ ,
  - 10:   Set  $k = k + 1$ .
  - 11: **end while**
- 



## 3. GLOBAL CONVERGENCE:

Examining the global convergence properties of the proposed approach, this section draws the following conclusions:

1. The sequence  $\Omega = \{u : u \in R^n, f(u) \leq f(u_1)\}$  is bounded within the level set of the objective function.
2. The inequality:

$$\|g(\tau) - g(v)\| \leq L \|\tau - v\|, \forall \tau, v \in R^n. \quad (3.1)$$

Holds for all  $\tau, v \in R^n$ , since the function  $g(u)$  is Lipschitz continuous with constant  $L > 0$  (see [5]).

**Theorem 3.1.** *A key property of Algorithm BBJ is that it always generates descent directions.*

*Proof.* By multiplying equation (8) by  $g_{\kappa+1}$  and using the  $\beta_{\kappa}^{BBJ}$  definition, we get

$$d_{\kappa+1}^T g_{\kappa+1} = -\|g_{\kappa+1}\|^2 + \frac{\|g_{\kappa+1}\|^2}{\alpha_{\kappa}(g_{\kappa}^T d_{\kappa})^2 / (1/2y_{\kappa}^T s_{\kappa} + (f_{\kappa+1} - f_{\kappa}) - g_{\kappa}^T s_{\kappa})} d_{\kappa}^T g_{\kappa+1}. \quad (3.2)$$

Essentially, it's:

$$d_{\kappa+1}^T g_{\kappa+1} = \frac{d_{\kappa}^T g_{\kappa+1} - [\alpha_{\kappa}(g_{\kappa}^T d_{\kappa})^2 / (1/2y_{\kappa}^T s_{\kappa} + (f_{\kappa+1} - f_{\kappa}) - g_{\kappa}^T s_{\kappa})] \|g_{\kappa+1}\|^2}{\alpha_{\kappa}(g_{\kappa}^T d_{\kappa})^2 / (1/2y_{\kappa}^T s_{\kappa} + (f_{\kappa+1} - f_{\kappa}) - g_{\kappa}^T s_{\kappa})}. \quad (3.3)$$

It may be inferred from this phrase that:

$$d_{\kappa+1}^T g_{\kappa+1} = \frac{\|g_{\kappa+1}\|^2}{\alpha_{\kappa}(g_{\kappa}^T d_{\kappa})^2 / (1/2y_{\kappa}^T s_{\kappa} + (f_{\kappa+1} - f_{\kappa}) - g_{\kappa}^T s_{\kappa})} g_{\kappa}^T d_{\kappa}. \quad (3.4)$$

Next:

$$d_{\kappa+1}^T g_{\kappa+1} = \beta_{\kappa}^{BBJ} g_{\kappa}^T d_{\kappa} < 0. \quad (3.5)$$

Verifying if the search's direction is indeed a fall descent.  $\square$

A key tool for examining global convergence is the Zoutendijk condition [28], often known as the Zoutendijk lemma, which verifies the stability and dependability of the CG algorithm by guaranteeing that its iterates approach a stationary point.

**Lemma 3.2.** *The following property is guaranteed if conditions (1) and (2) are satisfied when the step size  $\alpha_{\kappa}$  satisfies the Wolfe criteria and  $d_{\kappa}$  denotes a direction of descent:*

$$\sum_{\kappa \geq 0}^{\infty} \frac{(g_{\kappa}^T d_{\kappa})^2}{\|d_{\kappa}\|^2} < \infty. \quad (3.6)$$

**Theorem 3.3.** *If the assumptions are true and  $\{u_{\kappa}\}$  is generated by BBJ method. Then:*

$$\lim_{\kappa \rightarrow \infty} (\inf \|g_{\kappa}\|) = 0. \quad (3.7)$$

*Proof.* For every iteration  $\kappa$ , a positive scalar  $r > 0$  may be found such that the following condition is met if equation (3.7) is not true:

$$\|g_{\kappa+1}\| > r. \quad (3.8)$$

Once both sides have been squared and the search direction  $d_{\kappa+1} + g_{\kappa+1} = \beta_{\kappa} d_{\kappa}$  has been indicated, we get:

$$\|d_{\kappa+1}\|^2 + \|g_{\kappa+1}\|^2 + 2d_{\kappa+1}^T g_{\kappa+1} = (\beta_{\kappa})^2 \|d_{\kappa}\|^2. \quad (3.9)$$

The use of equations (3.5) through (3.9) implies the following:

$$\|d_{\kappa+1}\|^2 = \frac{(d_{\kappa+1}^T g_{\kappa+1})^2}{(d_{\kappa}^T g_{\kappa})^2} \|d_{\kappa}\|^2 - 2d_{\kappa+1}^T g_{\kappa+1} - \|g_{\kappa+1}\|^2. \quad (3.10)$$



Equation (3.10) is divided by  $(d_{\kappa+1}^T g_{\kappa+1})^2$  to yield:

$$\begin{aligned} \frac{\|d_{\kappa+1}\|^2}{(d_{\kappa+1}^T g_{\kappa+1})^2} &= \frac{\|d_{\kappa}\|^2}{(d_{\kappa}^T g_{\kappa})^2} - \frac{\|g_{\kappa+1}\|^2}{(d_{\kappa+1}^T g_{\kappa+1})^2} - \frac{2}{d_{\kappa+1}^T g_{\kappa+1}} \\ &\leq \frac{\|d_{\kappa}\|^2}{(d_{\kappa}^T g_{\kappa})^2} - \left( \frac{\|g_{\kappa+1}\|}{(d_{\kappa+1}^T g_{\kappa+1})} + \frac{1}{\|g_{\kappa+1}\|^2} \right) + \frac{1}{\|g_{\kappa+1}\|^2} \\ &\leq \frac{\|d_{\kappa}\|^2}{(d_{\kappa}^T g_{\kappa})^2} + \frac{1}{\|g_{\kappa+1}\|^2}. \end{aligned} \quad (3.11)$$

Thus, we get:

$$\frac{\|d_{\kappa+1}\|^2}{(d_{\kappa+1}^T g_{\kappa+1})^2} \leq \sum_{i=1}^{k+1} \frac{1}{\|g_i\|^2}. \quad (3.12)$$

Let for every  $k \in n$ , there exists  $c_1 > 0$  such that  $\|g_{\kappa}\| \geq c_1$  exists. Then:

$$\frac{\|d_{\kappa+1}\|^2}{(d_{\kappa+1}^T g_{\kappa+1})^2} < \frac{k+1}{c_1^2}. \quad (3.13)$$

Finally, we arrive at:

$$\sum_{\kappa=1}^{\infty} \frac{(g_{\kappa}^T d_{\kappa})^2}{\|d_{\kappa}\|^2} = \infty. \quad (3.14)$$

Similarly, as stated in Lemma 3.2, the condition  $\lim_{\kappa \rightarrow \infty} \inf \|g_{\kappa}\| = 0$  holds.  $\square$

#### 4. NUMERICAL EXPERIMENTS

Numerical experiments show that the New approach is successful in reducing salt-and-pepper noise. The performance of the New and FR techniques is evaluated on a PC using MATLAB R2017a. Both algorithms stop running as soon as the following conditions are met:

$$\frac{|f(u_{\kappa}) - f(u_{\kappa-1})|}{|f(u_{\kappa})|} \leq 10^{-4} \text{ and } \|f(u_{\kappa})\| \leq 10^{-4}(1 + |f(u_{\kappa})|). \quad (4.1)$$

In addition to a test picture and text sample, the experimental dataset includes common benchmark images such as MIR, CT, CerebSagE, and HeadCT. Using the Peak Signal-to-Noise Ratio (PSNR), the quality of the recovered pictures is measured in accordance with the methods used in [22, 26]. The following section describes the standards by which the efficacy of the restoration procedure is assessed:

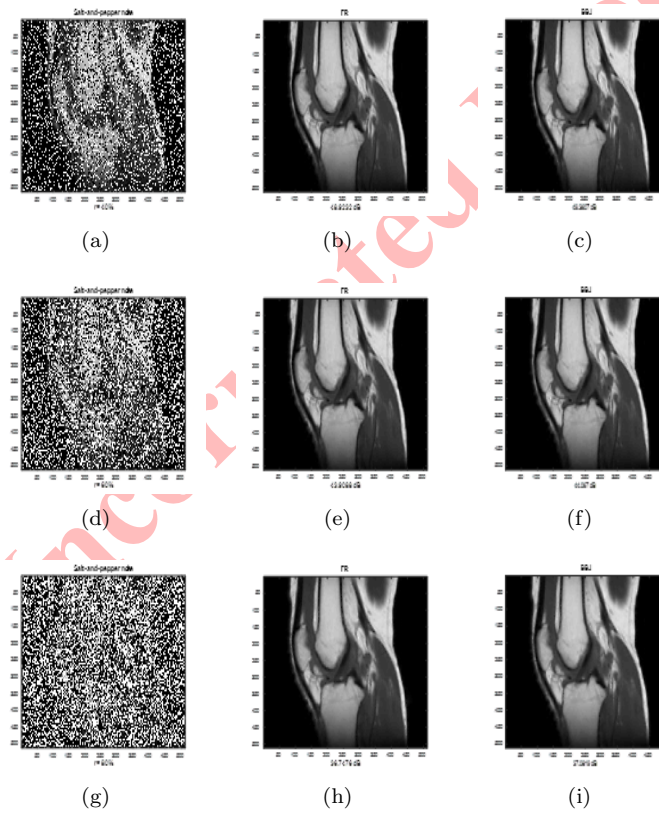
$$PSNR = 10 \log_{10} \frac{255^2}{\frac{1}{MN} \sum_{i,j} (u_{i,j}^r - u_{i,j}^*)^2}. \quad (4.2)$$

Denoting the original and restored image pixels as  $u_{i,j}^r$  and  $u_{i,j}^*$ , respectively, the study compares the proposed denoising algorithm with the FR method. Its speedier and more efficient behaviour is confirmed by the new algorithm's equivalent PSNR performance with fewer iterations and function evaluations. In an effort to strengthen the investigation's underlying theoretical framework, several research have looked at this subject from a variety of angles [1, 2, 11, 18, 20, 21]. As advancements observed in the field of Quasi-Newton techniques in [12, 13, 16, 19]



TABLE 1. Performance evaluation of the FR and BBJ algorithms based on numerical experiments.

Image	Noise level r (%)	FR-Method			BBJ-Method		
		NI	NF	PSNR (dB)	NI	NF	PSNR (dB)
MRI	40	52	68	48.9232	18	35	49.3607
	60	41	46	43.9088	17	34	44.0670
	80	62	111	36.7476	23	47	37.0819
CT	40	184	362	28.5833	59	123	28.7650
	60	228	454	26.5051	82	165	26.8454
	80	169	333	23.9568	77	158	24.2167
CerebSagE	40	153	291	36.2303	48	48	36.8706
	60	149	223	31.8960	47	47	32.3422
	80	333	645	25.5840	61	61	26.2162
HeadCT	40	2293	4577	8.7338	197	428	16.2261
	60	2421	4839	8.2760	227	490	14.9779
	80	2517	5029	7.8930	245	531	14.0644

FIGURE 1. Results obtained by applying the FR and BBJ algorithms to the MIR image with a resolution of  $256 \times 256$  pixels.

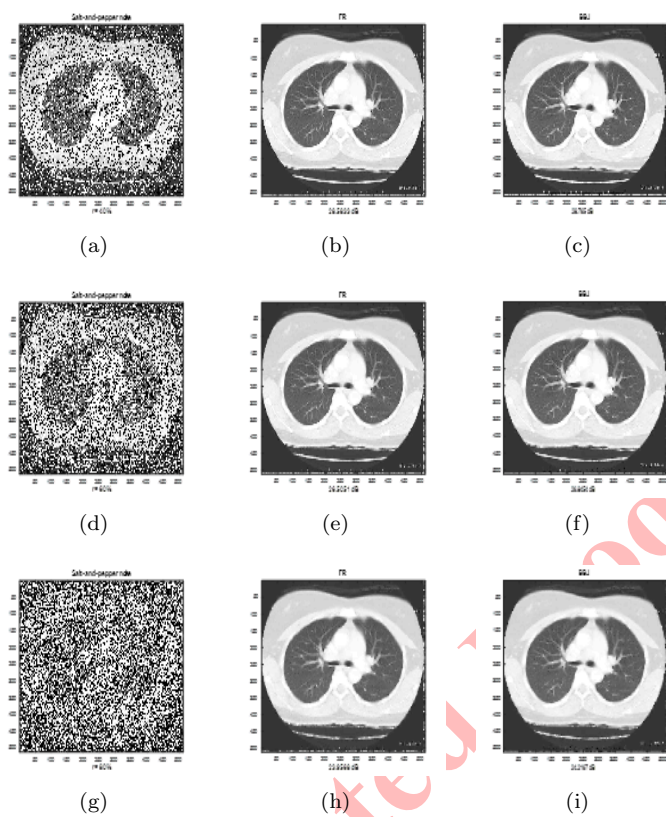


FIGURE 2. Results obtained by applying the FR and BBJ algorithms to the MIR image with a resolution of  $256 \times 256$  pixels.

Uncorrected Proof

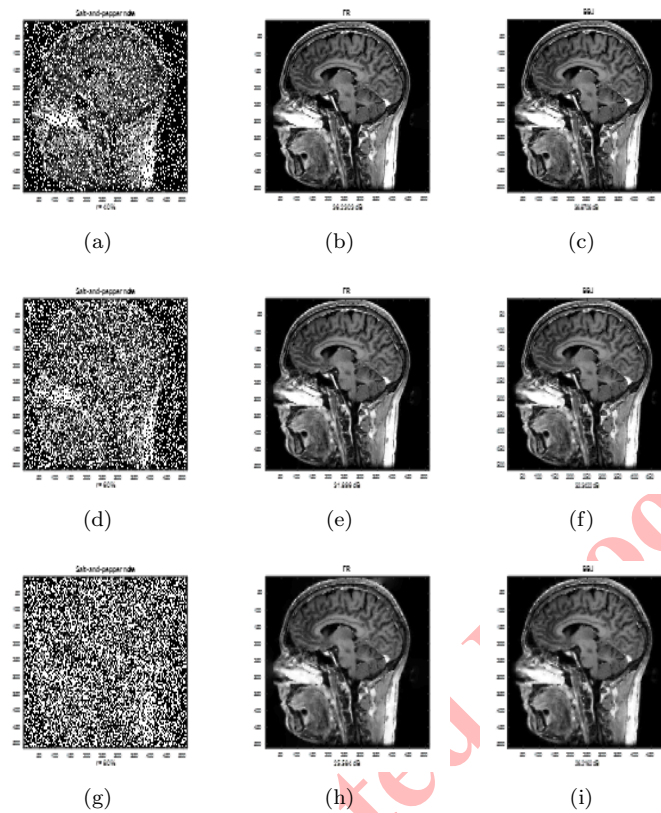


FIGURE 3. Results obtained by applying the FR and BBJ algorithms to the MIR image with a resolution of  $256 \times 256$  pixels.

## 5. CONCLUSIONS

To lessen impulse noise in digital pictures, a novel conjugate gradient formulation based on Taylor expansion has been put forth. Regardless of the parameter or line search option, the developed approach guarantees that the search direction always satisfies the descent condition. In mild circumstances, the BBJ algorithm achieves global convergence. Incorporating the traditional FR conjugate parameters into the BBJ structure yields promising results, as shown by comparative numerical studies. Overall, the quantitative results confirm the suggested approach's dependability and efficacy.

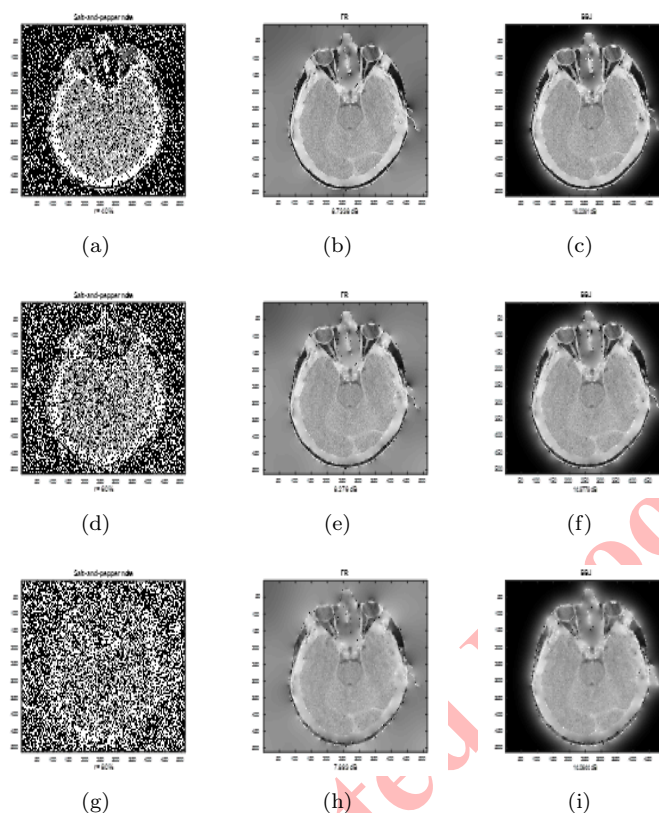


FIGURE 4. Results obtained by applying the FR and BBJ algorithms to the MIR image with a resolution of  $256 \times 256$  pixels.

#### REFERENCES

- [1] T. Ameen, M. Khalid, A. W. Abdulqahar, and A. Tariq, *Exploiting visual content for travel location recommendation*, In 2021 International Conference on Electrical, Computer and Energy Technologies (ICECET), (2021), 1–6.
- [2] T. Ameen and A. A. Ali, *Graph attention network for movie recommendation*, International Journal of Intelligent Engineering & Systems, *15*(3) (2022).
- [3] J. F. Cai, R. H. Chan, and B. Morini, *Minimization of an edge-preserving regularization functional by conjugate gradient type methods*, in Mathematics and Visualization: Image Processing Based on Partial Differential Equations, Springer, (2007), 1–7.
- [4] Y. H. Dai and Y. Yuan, *A nonlinear conjugate gradient method with a strong global convergence property*, SIAM Journal on Optimization, *10*(1) (1999), 177–182.
- [5] Y. H. Dai, J. Han, G. Liu, D. Sun, H. Yin, and Y. Yuan, *Convergence properties of nonlinear conjugate gradient methods*, SIAM Journal on Optimization, *10*(2) (1999), 345–358.
- [6] R. Fletcher and C. M. Reeves, *Function minimization by conjugate gradients*, The Computer Journal, *7*(2) (1964), 149–154.
- [7] W. W. Hager and H. Zhang, *A new conjugate gradient method with guaranteed descent and an efficient line search*, SIAM Journal on Optimization, *16*(1) (2005), 170–192.
- [8] B. A. Hassan and A. A. A. Abdullah, *Improvement of conjugate gradient methods for removing impulse noise images*, Indonesian Journal of Electrical Engineering and Computer Science, *29*(1) (2023), 245–251.

- [9] B. A. Hassan and H. A. Alashoor, *On image restoration problems using new conjugate gradient methods*, Indonesian Journal of Electrical Engineering and Computer Science, *29*(3) (2023), 1438–1445.
- [10] B. A. Hassan and H. A. Alashoor, *A new type coefficient conjugate on the gradient methods for impulse noise removal in images*, European Journal of Pure and Applied Mathematics, *15*(4) (2022), 2043–2053.
- [11] B. A. Hassan, F. Alfarag, and S. Djordjevic, *New step sizes of the gradient methods for unconstrained optimization problem*, Italian Journal of Pure and Applied Mathematics, (2021).
- [12] B. A. Hassan, F. Alfarag, A. Ibrahim, and A. Abubakar, *An improved quasi-Newton equation on the quasi-Newton methods for unconstrained optimizations*, Indonesian Journal of Electrical Engineering and Computer Science, *22*(2), 389–397.
- [13] B. A. Hassan and M. A. A. Kahya, *A new class of quasi-Newton updating formulas for unconstrained optimization*, Journal of Interdisciplinary Mathematics, *24*(8) (2022), 2355–2366.
- [14] B. A. Hassan and H. M. Sadiq, *A new formula on the conjugate gradient method for removing impulse noise images*, Bulletin of the South Ural State University, Series Mathematical Modelling, Programming and Computer Software, *15*(4) (2022), 123–130.
- [15] B. A. Hassan and H. M. Sadiq, *Efficient new conjugate gradient methods for removing impulse noise images*, European Journal of Pure and Applied Mathematics, *15*(4) (2022), 2011–2021.
- [16] B. A. Hassan and R. M. Sulaiman, *A new class of self-scaling for quasi-Newton method based on the quadratic model*, Indonesian Journal of Electrical Engineering and Computer Science, *21*(3) (2021), 1830–1836.
- [17] B. A. Hassan, *A new formula for conjugate parameter computation based on the quadratic model*, Indonesian Journal of Electrical Engineering and Computer Science, *3* (2019), 954–961.
- [18] B. A. Hassan, *A modified quasi-Newton methods for unconstrained optimization*, Italian Journal of Pure and Applied Mathematics, *42* (2019), 1–8.
- [19] B. A. Hassan, *A modified quasi-Newton methods for unconstrained optimization*, Italian Journal of Pure and Applied Mathematics, *42* (2019).
- [20] H. N. Jabbar, Y. J. Subhi, H. N. Hussein, and B. A. Hassan, *Solving single variable functions using a new secant method*, Journal of Interdisciplinary Mathematics, *28*(1) (2025), 245–251.
- [21] A. M. Jasim, Y. J. Subhi, and B. A. Hassan, *On new secant-method for minimum functions of one variable*, Journal of Interdisciplinary Mathematics, *28*(1) (2025), 291–296.
- [22] X. Jian and J. Jinbao, *A sufficient descent Dai–Yuan type nonlinear conjugate gradient method for unconstrained optimization problems*, Nonlinear Dynamics, *72*(1–2) (2013), 101–112.
- [23] Y. Nishida and H. Iiduka, *Conjugate gradient methods using value of objective function for unconstrained optimization*, Optimization Letters, *6*(5) (2011), 941–955.
- [24] J. Nocedal and S. J. Wright, *Numerical Optimization*, Springer, 2006.
- [25] E. Polak and G. Ribiere, *Note sur la convergence de directions conjugate*, Revue Française d’Informatique et de Recherche Opérationnelle, *16* (1969), 35–43.
- [26] X. Wei, R. Junhong, Z. Xiao, L. Zhi, and L. Yueyong, *A new DY conjugate gradient method and applications to image denoising*, IEICE Transactions on Information and Systems, *E101-D*(12) (2018), 2984–2990.
- [27] G. Yu, J. Huang, and Y. Zhou, *A descent spectral conjugate gradient method for impulse noise removal*, Applied Mathematics Letters, *23*(5) (2010), 555–560.
- [28] G. Zoutendijk, *Nonlinear programming: computational methods*, in Integer and Nonlinear Programming, North-Holland, 1970, 37–86.

